34th Annual International Conference of the IEEE EMBS
San Diego, California USA, 28 August - 1 September, 2012

A Convolution Based Method for Calculating Inputs from Dendritic Fields in a Continuum Model of the Retina

Amr Al Abed, Shijie Yin, Gregg J. Suaning, *Member, IEEE*, Nigel H. Lovell, *Fellow, IEEE*, Socrates Dokos, *Member, IEEE*

***Abstract*—Computational models are valuable tools that can be used to aid the design and test the efficacy of electrical stimulation strategies in prosthetic vision devices. In continuum models of retinal electrophysiology, the effective extracellular potential can be considered as an approximate measure of the electrotonic loading a neuron's dendritic tree exerts on the soma. A convolution based method is presented to calculate the local spatial average of the effective extracellular loading in retinal ganglion cells (RGCs) in a continuum model of the retina which includes an active RGC tissue layer. The method can be used to study the effect of the dendritic tree size on the activation of RGCs by electrical stimulation using a hexagonal arrangement of electrodes (hexpolar) placed in the suprachoroidal space.**

I. Introduction

SEVERAL groups around the world are pursuing the development of visual prosthesis to aid patients with retinitis pigmentosa and age-related macular degeneration [1-3], two of the most prevalent retinal diseases and leading causes of blindness in developed countries [4]. Both of these diseases result in degeneration of the retina, predominantly the outer retina where the photoreceptors are located, leading to eventual loss of vision. The inner retina however is largely left intact, even in patients who have been clinically blind for many years [5, 6], raising the possibility that these inner retinal neurons can be electrically stimulated to elicit light perception [7, 8].

Computational modeling is a valuable tool for quantitative analysis of the function of biological systems under healthy and diseased conditions and to aid in the design of vision prosthesis and the development of optimal signal processing and stimulation strategies for use in such devices.

Initial modeling studies on the effects of electrical stimulation of the retina have been limited in their scope [9, 10] focusing on the responses of retinal ganglion cells (RGCs) to electrical stimulation and have largely ignored the presence of the rest of the retinal network and passive propagation through retinal layers. Other groups have attempted to incorporate these presynaptic inputs by modeling the retina as a discrete network [11, 12].

Our group has developed a continuum model of the retinal network which includes both passive retinal neuronal properties and active ganglion cell behavior. The generalized retinal network model of the ON system, the visual pathway that responds to light stimuli that are brighter than the background, incorporates synaptic inputs from bipolar and amacrine cells to RGCs to modulate the spiking activity of RGCs as it occurs physiologically. The model was used to simulate both epiretinal and suprachoroidal electrical stimulation of the retina using bipolar electrodes as well as the responses to light stimulation [13, 14].

These studies indicate that the retinal network effects play a significant role in shaping the spiking activity of the RGC layer and therefore it is hypothesized that it will affect the spatial and temporal responses to excitation at the cortical level. Therefore the extent of neural connections in the retinal and the dendritic trees of its component cells will be paramount in modulating these responses. In this paper a convolution based method for calculating the electrotonic (passive RC) input from dendritic trees of RGCs to their soma is presented. This pilot study suggests that the convolution integral is a promising method to evaluate electrical input experienced by each cell following electrical stimulation in continuum models of the retina.

II. Methods

A 3D finite-element continuum model of electrical stimulation of a retina that lies between choroid and vitreous fluid layers is described (Fig. 1) using COMSOL Multiphysics Version 4.2a (COMSOL AB, Sweden). The model consists of both an active neural retinal layer comprising RGCs as well as passive conductive layers including the inner plexiform layer (IPL), inner nuclear layer (INL), outer plexiform layer (OPL), outer nuclear layer (ONL), sub retinal space (modeled with cone photoreceptors), retinal pigment epithelium (RPE) and choroid. The conductivities of various layers were largely derived from [15].

A hexagonal arrangement of circular disc electrodes (0.2 mm in radius) are placed on the top boundary of the choroid layer, 426 μm from the retinal pigment epithelium to achieve suprachoroidal stimulation. This distance is based on an *in vivo* measurement of choroid thickness from a human retina [16]. The central disc is the active electrode and surrounding discs electrodes are the return electrodes. Current can be returned at one or all six surrounding electrodes by connecting the return electrode(s) to ground.

This research was supported by the Australian Research Council (ARC) through its Special Research Initiative (SRI) in Bionic Vision Science and Technology grant to Bionic Vision Australia (BVA).

A. Al Abed, S. Yin, N. H. Lovell and G. J. Suaning, and S. Dokos are with the Graduate School of Biomedical Engineering, University of New South Wales, Sydney, NSW 2052, Australia (email: s.dokos@ unsw.edu.au).

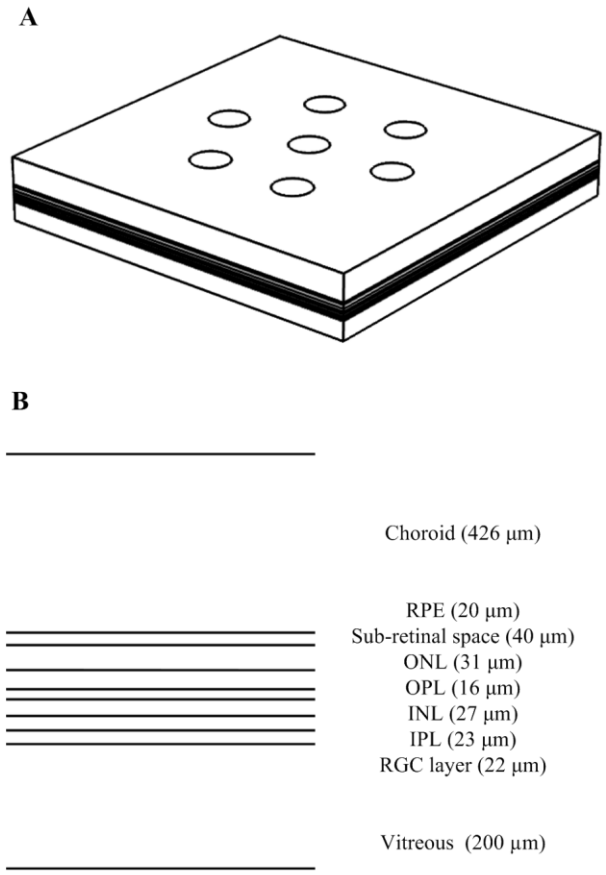

Fig. 1. A. Schematic diagram of the retinal model with hexagonally arranged electrodes. Current is injected at the center electrode and returned at the peripheral electrodes. The radius of each electrode is 0.2 mm and the distance between centers of central electrode and each of the peripheral electrodes is 1 mm. B. Slice through the various layers of the model with the thickness of each layer.

The extracellular voltage distribution V_e (V) within the passive conductance regions was governed by Poisson's equation

$$\nabla \cdot (-\sigma \nabla V_e) = I \tag{1}$$

where σ (S/m) is the conductivity of the bulk vitreous medium and I is the volume current density source (A/m^3) injected into the vitreous at the central electrode.

Within the active RGC region, an adaptation of the bidomain equations was applied (Fig. 2).

A simplified model the spatial morphology of neurons in the continuum model was implemented by tying the intracellular potential V_i (V), of each cell to a resting potential V_r (V), representing the intracellular potential in the more distal portions of the neuron (axon and dendrites). This tie is achieved using a resistor and as a consequence, the intracellular potential is not able to float freely with changes in the surrounding extracellular potential during extracellular stimulation. The extracellular, but not intracellular, potential was continuous across elements in the finite element model to allow for local excitation and activation of individual ganglion cells without spread of activation to neighboring cells, important for eliciting focal excitation of phosphenes.

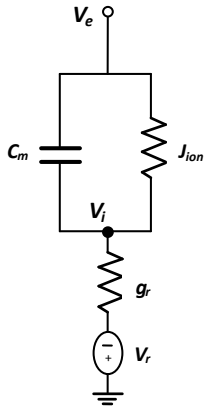

Fig. 2. RC circuit of the active RGC membrane potential. C_m represents the membrane capacitance, V_e is the extracellular potential, J_{ion} is the ionic current per unit area through gated channels in the cell's soma, and g_r is the resistive tie connecting the intracellular potential V_i to a resting potential V_r, R_m is the specific membrane resistance.

The extracellular voltage is determined from

$$\sigma_e \nabla^2 V_e = -I_m \tag{2}$$

where the extracellular retinal conductivity σ_e of the remaining layers are derived from [18, 19], and I_m is the RGC membrane current density per unit volume, given by

$$I_m = C_m \frac{\partial V_m}{\partial t} + J_{ion} = g_r (V_r - V_i + EffV_e) \tag{3}$$

and V_m is the transmembrane potential given by

$$V_m = V_i - V_e \tag{4}$$

C_m is the membrane capacitance and is 1 μF/cm^2 for all cell types, consistent with previous modeling [9] and experimental studies [17]. β denotes the surface to volume ratio of the ganglion cell layer. A β value of 9.25x10^{-4} m^{-1} was arrived at by assuming a ganglion cell density of 2000 cells/mm^2 [18], that the cells are spherical with a soma diameter of 18 μm and that extracellular currents stimulate only the soma of the ganglion cell [11] as threshold for activation is lowest near the soma or axon hillock [10].

J_{ion} is determined based on the ionic formulation of Fohlmeister and Miller [9]. The extracellular voltage gradient is suggested to contribute to the generation of neural action potentials and could represent the difference in potential between distal portions of the neuron, representing the extent of synaptic inputs, and the soma. At each time step, a convolution integral was used to calculate the average effective extracellular potential ($EffV_e$) within a defined volume surrounding each RGC_i.

$$EffV_e = V_e - \frac{1}{n} \iiint V_e \left(\left((x-x_i)^2 + (y-y_i)^2 + (z-z_i)^2 \right) < r^2 \right) dxdydz \tag{5}$$

It is assumed that a sphere with radius r (m) represents the dendritic field and n the number of finite elements within the sphere. Hence $EffV_e$ (V) is an approximation of the extent of the synaptic input electrotonic input received by the soma.

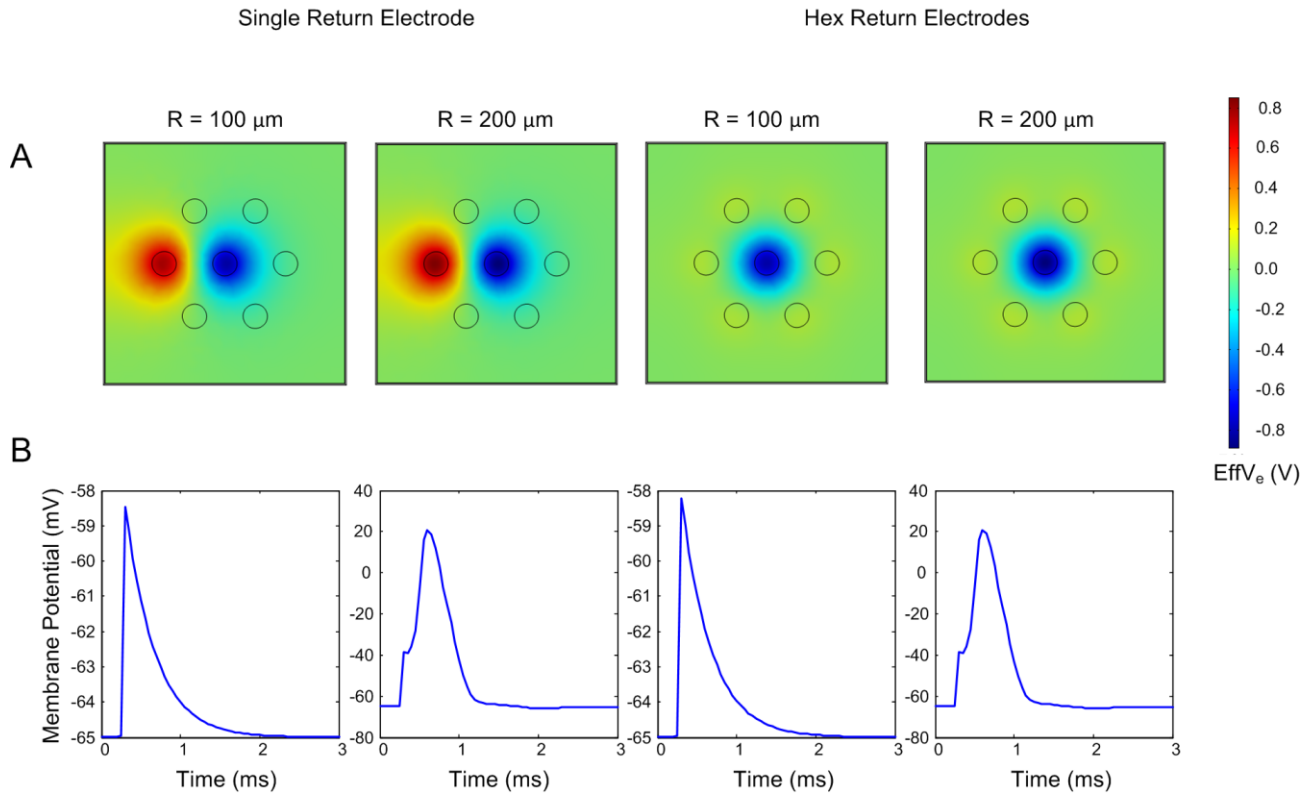

Fig. 3 Simulation results using a combination of two dendritic field sizes and return electrode configurations. A. Effective V_e distribution profiles measured at the end of the stimulus pulse (0.5-0.6 ms). B. Membrane potential observed at a point below the centre of the central stimulating electrode.

III. Results

Simulation results are shown in Fig. 3 for a combination of return electrodes and "r" values in the convolution integral (equation 5). The membrane potential of a point representing an RGC cell and lying directly below the central stimulating electrode was probed for active excitation following electrical stimulation using a pulse 0.2 ms in duration and a monophasic cathodic pulse 6.3 mA in amplitude. Action potentials were elicited when the size of the dendritic field was 200 µm regardless of whether a single electrode (bipolar) or six hexagonally arranged electrodes (hexpolar) were used as ground electrodes (Fig. 3B). Passive electrotonic responses were recorded when the size of the dendritic field was set to 100 µm (Fig. 3B).

Maps of the effective V_e are presented at the end of the stimulus pulse for all simulation setups (Fig. 3A). Although the general pattern of distribution of V_e appears to be identical between simulations using a single return electrode or hexagonal return electrodes, the value of V_e measured at a point directly below the center of the stimulus electrode is slightly different which could explain why RGC action potentials were triggered when a larger dendritic field was used in the convolution integral. When the radius was 100 µm, V_e was -0.79 V and -0.78 V for single and hexagonal return electrodes respectively. However when the radius was increased to 200 µm, V_e increased to -0.88 V and -0.87 V for bipolar and hexpolar return configurations respectively.

IV. Discussion

The continuum approach is used extensively in cardiac electromechanical [19] and smooth muscle and gastrointestinal electrophysiology [20] modeling. However its use in neuronal modeling is less widely adopted because, in general, neurons are not connected by gap junctions and therefore neuronal networks do not behave as an electric syncytium like cardiac or smooth muscle tissue. The presence of gap junctions allows modeling of syncytium tissues using either the bidomain or monodomain formulation of the cable equation of electric propagation and this will determine the electrotonic input experienced by each cell/element from adjacent cells/elements. However in the case of neural networks a single neuron may receive input from a number of neurons depending on the size and morphology of its dendritic tree and the types of synaptic inputs it receives. Therefore when implementing finite element neuronal models the electrotonic loading on any particular element should not be set to be received strictly from adjacent elements. The traditional approaches of using compartmental discrete models (e.g. [21, 22]) and Cajal branching patterns [23] to simulate dendrites of neurons cannot be easily applied in continuum electrophysiology

modeling. Therefore there is a need to develop numerical algorithms to estimate dendritic fields and synaptic connections in continuum electrophysiology models.

Towards this aim a convolution based method is described and implemented in a continuum model of electrical stimulation of the retina which has an active RGC layer and conductive layers describing other retinal layers.

The effective potential gradient of RGCs is estimated using a convolution integral to calculate the average extracellular potential at distal ends of the neuron. The dendritic tree is assumed to be spherical around the soma. Electrical stimulation was delivered using circular electrodes in the suprachoroidal space. Either a single or six electrodes arranged in a hexagonal pattern around the stimulating electrode were set as ground electrodes. The volume of the convolution integral determines the size of the dendritic field and thus the effective extracellular potential gradient and electrotonic input into each RGC's soma which in turn determines whether there is sufficient excitatory input to trigger an action potential in RGCs.

The threshold for excitation is found to be higher when a convolution integral is used to estimate the dendritic field compared to using a weighted average of four points surrounding the soma as previously used by our group.

V. Conclusion

This is a preliminary study to test the feasibility of implementing a convolution integral approach to calculate the effective extracellular gradient experienced by the dendritic tree of each RGC cell in a retinal continuum model. Future work includes incorporation of this approach in a continuum network model of the retina with synaptic connections between different neuron types in the network. In addition, future work will involve updating the thickness of various retinal layers in the model to reflect changes that occur during disease. This will enable more realistic representation of retinal neuronal circuitry and thus help in testing the efficacy of various stimulation strategies used in vision prosthetic devices.

References

[1] J. Wyatt and J. F. Rizzo, "Ocular implants for the blind," *IEEE Spectr.,* pp. 47-53, 1996.

[2] H. Sakaguchi, T. Fujikado, X. Fang, H. Kanda, M. Osanai, K. Nakauchi, Y. Ikuno, M. Kamei, T. Yagi, S. Nishimura, M. Ohji, and Y. Tano, "Transretinal electrical stimulation with a suprachoroidal multichannel electrode in rabbit eyes," *Jpn J Ophthalmol,* vol. 48, pp. 256-61, May-Jun 2004.

[3] Y. T. Wong, S. C. Chen, J. M. Seo, J. W. Morley, N. H. Lovell, and G. J. Suaning, "Focal activation of the feline retina via a suprachoroidal electrode array," *Vision Res,* vol. 49, pp. 825-33, Mar 2009.

[4] C. C. Klaver, R. C. Wolfs, J. R. Vingerling, A. Hofman, and P. T. de Jong, "Age-specific prevalence and causes of blindness and visual impairment in an older population: the Rotterdam Study," *Arch Ophthalmol,* vol. 116, pp. 653-8, May 1998.

[5] A. Santos, M. S. Humayun, E. de Juan, Jr., R. J. Greenburg, M. J. Marsh, I. B. Klock, and A. H. Milam, "Preservation of the inner retina in retinitis pigmentosa. A morphometric analysis," *Arch Ophthalmol,* vol. 115, pp. 511-5, Apr 1997.

[6] J. L. Stone, W. E. Barlow, M. S. Humayun, E. de Juan, Jr., and A. H. Milam, "Morphometric analysis of macular photoreceptors and ganglion cells in retinas with retinitis pigmentosa," *Arch Ophthalmol,* vol. 110, pp. 1634-9, Nov 1992.

[7] M. S. Humayun, E. de Juan, Jr., G. Dagnelie, R. J. Greenberg, R. H. Propst, and D. H. Phillips, "Visual perception elicited by electrical stimulation of retina in blind humans," *Arch Ophthalmol,* vol. 114, pp. 40-6, Jan 1996.

[8] J. F. Rizzo, 3rd, J. Wyatt, J. Loewenstein, S. Kelly, and D. Shire, "Methods and perceptual thresholds for short-term electrical stimulation of human retina with microelectrode arrays," *Invest Ophthalmol Vis Sci,* vol. 44, pp. 5355-61, Dec 2003.

[9] J. F. Fohlmeister and R. F. Miller, "Impulse encoding mechanisms of ganglion cells in the tiger salamander retina," *J Neurophysiol,* vol. 78, pp. 1935-47, Oct 1997.

[10] R. J. Greenberg, T. J. Velte, M. S. Humayun, G. N. Scarlatis, and E. de Juan, Jr., "A computational model of electrical stimulation of the retinal ganglion cell," *IEEE Trans Biomed Eng,* vol. 46, pp. 505-14, May 1999.

[11] N. P. Cottaris and S. D. Elfar, "How the retinal network reacts to epiretinal stimulation to form the prosthetic visual input to the cortex," *J Neural Eng,* vol. 2, pp. S74-90, Mar 2005.

[12] J. Teeters, A. Jacobs, and F. Werblin, "How neural interactions form neural responses in the salamander retina," *J Comput Neurosci,* vol. 4, pp. 5-27, Jan 1997.

[13] S. Yin, N. H. Lovell, G. J. Suaning, and S. Dokos, "Continuum model of light response in the retina," *Conf Proc IEEE Eng Med Biol Soc,* vol. 2011, pp. 908-11, 2011.

[14] S. Yin, N. H. Lovell, G. J. Suaning, and S. Dokos, "A continuum model of the retinal network and its response to electrical stimulation," *Conf Proc IEEE Eng Med Biol Soc,* vol. 2010, pp. 2077-80, 2010.

[15] C. J. Karwoski and X. Xu, "Current source-density analysis of light-evoked field potentials in rabbit retina," *Vis Neurosci,* vol. 16, pp. 369-77, Mar-Apr 1999.

[16] J. S. Brown, D. I. Flitcroft, G. S. Ying, E. L. Francis, G. F. Schmid, G. E. Quinn, and R. A. Stone, "In vivo human choroidal thickness measurements: evidence for diurnal fluctuations," *Invest Ophthalmol Vis Sci,* vol. 50, pp. 5-12, Jan 2009.

[17] P. A. Coleman and R. F. Miller, "Measurement of passive membrane parameters with whole-cell recording from neurons in the intact amphibian retina," *J Neurophysiol,* vol. 61, pp. 218-30, Jan 1989.

[18] C. W. Oyster, E. S. Takahashi, and D. C. Hurst, "Density, soma size, and regional distribution of rabbit retinal ganglion cells," *J Neurosci,* vol. 1, pp. 1331-46, Dec 1981.

[19] A. V. Panfilov and A. V. Holden, *Computational biology of the heart*. Chichester ; New York: Wiley, 1997.

[20] P. Du, G. O'Grady, J. B. Davidson, L. K. Cheng, and A. J. Pullan, "Multiscale modeling of gastrointestinal electrophysiology and experimental validation," *Crit Rev Biomed Eng,* vol. 38, pp. 225-54, 2010.

[21] G. A. Enciso, M. Rempe, A. V. Dmitriev, K. E. Gavrikov, D. Terman, and S. C. Mangel, "A model of direction selectivity in the starburst amacrine cell network," *J Comput Neurosci,* vol. 28, pp. 567-78, Jun 2010.

[22] T. Radman, A. Datta, R. L. Ramos, J. C. Brumberg, and M. Bikson, "One-dimensional representation of a neuron in a uniform electric field," *Conf Proc IEEE Eng Med Biol Soc,* vol. 2009, pp. 6481-4, 2009.

[23] H. Cuntz, F. Forstner, A. Borst, and M. Hausser, "One rule to grow them all: a general theory of neuronal branching and its practical application," *PLoS Comput Biol,* vol. 6, 2010.